Pure Appl. Chem., Vol. 77, No. 2, pp. 391–398, 2005.
DOI: 10.1351/pac200577020391
© 2005 IUPAC

Control of deposition profile of Cu for large-scale integration (LSI) interconnects by plasma chemical vapor deposition*

Kosuke Takenaka, Masaharu Shiratani‡, Manabu Takeshita, Makoto Kita, Kazunori Koga, and Yukio Watanabe

Department of Electronics, Kyushu University, Fukuoka, Japan

Abstract: H-assisted plasma chemical vapor deposition (HAPCVD) realizes control of deposition profile of Cu in trenches. The key to the control is ion irradiation to surfaces. With increasing the flux and energy of ions, the profile changes from conformal to subconformal and then to an anisotropic one, for which Cu material is filled from the bottom of the trench without deposition on the sidewall. H_3^+ and ArH^+ are identified as the major ionic species which contribute to the control, and hence the deposition profile also depends on a ratio $R = H_2/(Ar + H_2)$.

Keywords: Cu interconnects; plasma chemical vapor deposition; deposition profile; anisotropy; trench.

INTRODUCTION

Control of deposition profile in trenches and holes becomes important for fabrication of nanostructures such as ultra large-scale integration (ULSI) interconnects, quantum dots and wires, and micro-electro-chemical systems [1]. Although Cu interconnects in ULSI have been fabricated by seed-layer deposition using physical vapor deposition (PVD) and subsequent filling using electroplating, the former deposition becomes difficult owing to reduction in the feature size of trenches and via holes [2,3]. PVD usually results in subconformal deposition profile in trenches. For a narrow trench of a high aspect ratio, such subconformal deposition results in a keyhole in the trench. Plasma [4–9] and thermal chemical vapor depositions (CVDs) [10–17] realize conformal filling in trenches. The conformal filling, however, results in a small crystal grain size below half of the trench width and also in a seam where impurities of high concentration remain. To solve these problems associated with the conformal filling, we have proposed anisotropic deposition, for which Cu material is filled preferentially from the bottom of trenches and via holes. In our previous experiments for the anisotropic deposition, deposition was observed on the sidewall as well as top and bottom, and hence small trenches were pinched off [18]. Recently, we have succeeded in suppressing such sidewall deposition, by using a H-assisted plasma chemical vapor deposition (HAPCVD) in which argon gas is added to H_2 gas. Using this method, we have realized not only subconformal and conformal deposition profiles but also an anisotropic one, for which Cu material is filled from the bottom of a trench without deposition on the sidewall. In this paper, we will report on a series of results concerning Cu deposition using HAPCVD with focus on the effects of gas mixture ratio $R = H_2/(H_2 + Ar)$ on the deposition profiles.

*Paper based on a presentation at the 16th International Symposium on Plasma Chemistry (ISPC-16), Taormina, Italy, 22–27 June 2003. Other presentations are published in this issue, pp. 345–495.

‡Corresponding author

EXPERIMENTAL DETAILS

Experiments were performed using a capacitively coupled parallel-plate reactor with a H atom source [4–9]. This reactor provides independent control of concentrations of Cu-containing radicals and H atoms. A schematic diagram of the reactor is shown in Fig. 1. For the main discharge, the mesh (14 mesh/inch) powered electrode of 85 mm in diameter and the plane substrate electrode of 85 mm in diameter were placed at a distance of 42 mm. The discharge of H atom source was sustained with a radio frequency (rf) induction coil of 100 mm in diameter placed at 75 mm above the substrate electrode of the main discharge. The electrodes for the main discharge and the coil for the H atom source, which were made of stainless steel and copper, respectively, were installed in a grounded stainless steel vessel of 250 mm in inner diameter and 315 mm in height. The H atom source was electrically separated from the main discharge region using a grounded mesh (30 mesh/inch) of 250 mm in diameter placed at 30 mm below the rf coil and 3 mm above the rf electrode for the main discharge. The excitation frequency used for the main discharge was 28 MHz and the supplied power P_m was below 30 W, whereas the excitation frequency used for the H atom source was 13.56 MHz and the supplied power P_{as} was below 150 W.

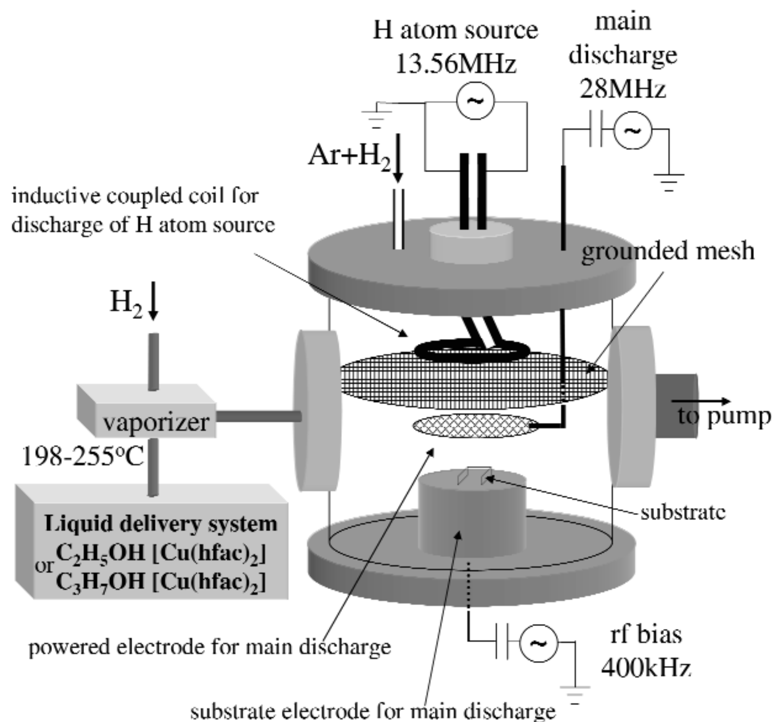

Fig. 1 Schematic diagram of HAPCVD reactor.

A Si substrate with trenches, which was covered with a WN film of 50 nm in thickness as a diffusion barrier for Cu, was placed on the substrate electrode for the main discharge, and the substrate temperature T_s was kept at 130 or 150 °C. An rf voltage of 400 kHz was applied to the substrate to provide the direct current (dc) bias voltage V_{dc} in a range of –200 to 0 V.

The source material for Cu deposition used was Cu(hfac)$_2$, bis(1,1,1,5,5,5, hexafluoroacetylacetonato)Cu(II), dissolved in ethanol (C_2H_5OH) or propanol (C_3H_7OH) at a concentration of 0.1–1.1 mol/l. The material was vaporized at a temperature of 195 to 255 °C, and then transported to the reactor at a flow rate of 4.5–36 sccm together with H_2 carrier gas supplied at a flow rate of 10 sccm.

In addition, Ar + H_2 (0–100 %) gases were supplied at a flow rate of 80–170 sccm to the H atom source. The total pressure of the reactor was 13 Pa.

Intensity measurements of optical emissions from the main discharge were performed using an optical detection system, which consisted of a lens and a 24-cm polychromator with an intensified multichannel detector. Ion saturation current in the main discharge was measured with a Langmuir probe at 12 mm above the center of the substrate electrode. Ionic species, which impinge on the substrate surface, were identified with a quadrupole mass spectrometer (Q-mass: Hiden EQP 500) mounted under the substrate electrode. Thickness and deposition profile of Cu in trenches were evaluated with a scanning electron microscope (SEM: JEOL JSM-6320FZ). Electrical conductivity of Cu films was analyzed by the four-point probe method.

RESULTS AND DISCUSSION

Deposition profile in trenches

First, we observed deposition profiles in trenches using cross-sectional SEM images. Typical images are shown in Figs. 2a–c. The HAPCVD reactor realizes various profiles: (Fig. 2a) conformal, (Fig. 2b) subconformal, and (Fig. 2c) anisotropic ones. The conformal profile is obtained when the flux and kinetic energy of ions impinging on the surface are so small that ions have little effects on the deposition.

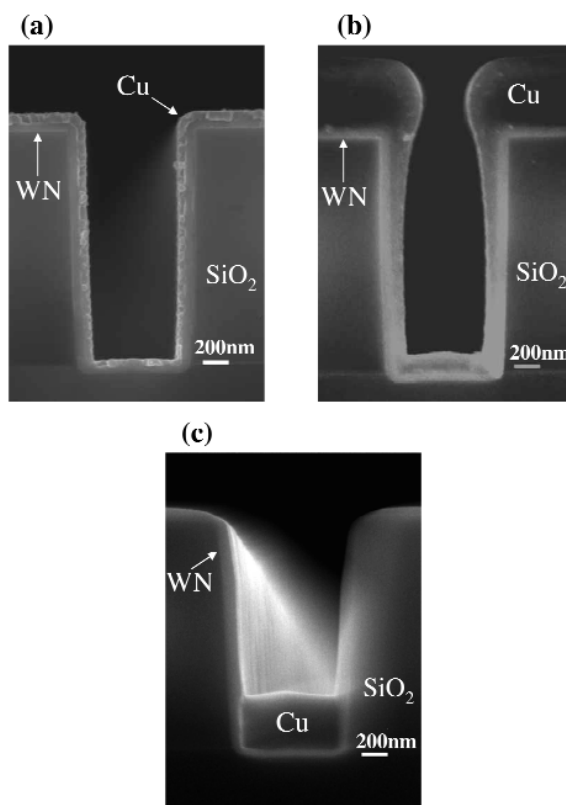

Fig. 2 Cross-sectional SEM images of Cu films in trench for (a) conformal, (b) subconformal, and (c) anisotropic depositions. Deposition condition: $C_2H_5OH[Cu(hfac)_2$:0.146 mol/l] = 18 sccm, H_2 = 45 sccm, 8 Pa, P_m = 10 W, P_{as} = 150 W, V_{dc} = 0 V, and T_s = 130 °C. $C_3H_7OH[Cu(hfac)_2$:0.84 mol/l] = 18 sccm, H_2 = 180 sccm, 24 Pa, P_m = 50 W, P_{as} = 150 W, V_{dc} = 0 V, and T_s = 130 °C. $C_2H_5OH[Cu(hfac)_2$:0.146 mol/l] = 4.5 sccm, Ar + H_2 (33 %) = 90 sccm, 13 Pa, P_m = 45 W, P_{as} = 150 W, V_{dc} = –150 V, and T_s = 150 °C.

Such deposition condition is realized using the main discharge of a low power density (≤0.1 Wcm^{-2}) without applying the substrate bias voltage or using the triode configuration [18], for which the ion flux is significantly reduced owing to a grounded mesh placed above the substrate. The subconformal profile tends to be obtained using the main discharge of a relatively high power density (>0.4 Wcm^{-2}) without the substrate bias voltage. The anisotropic profile is realized with the main discharge of a relatively high power density (>0.4 Wcm^{-2}) with the substrate bias voltage. The anisotropy, which is defined as a ratio of film thickness on the bottom surface of a trench to that on its sidewall, can be enhanced considerably by increasing the flux and kinetic energy of ions [18].

Next, we studied the deposition rate on the top and bottom surfaces and sidewall of a trench as a function of ratio $R = H_2/(H_2 + Ar)$ for a substrate bias voltage corresponding to a sheath voltage $V_{sheath} = -114$ V, since the sputtering due to heavy ions such as Ar^+ and ArH^+ easily modifies the deposition profile. Figure 3 shows the results for trenches 0.5 μm wide and 2.2 μm deep. The deposition rates on the top and bottom surfaces tend to decrease with increasing R, resulting in zero for $R \geq 66$ % and $R \geq 82$ %, respectively. On the other hand, no disposition on the sidewall takes place for $R > 11$ %. Cu is deposited only on the bottom surface for $R = 66$ %, which is a promising feature that may realize ULSI processes without chemical mechanical polishing. The deposition rate on the bottom surface is higher than that on the top surface for $R = 33$–66 %, whereas the opposite result is obtained for $R = 11$ %. Although nothing is deposited on all surfaces of trenches for $R = 100$ % in Fig. 3, Cu deposition on them is observed in the case of no substrate bias voltage (not shown here).

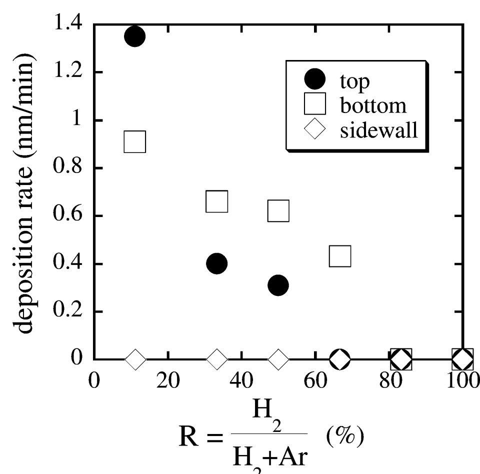

Fig. 3 $R = H_2/(H_2 + Ar)$ ratio dependence of deposition rate at top and bottom surfaces of trenches 0.5 μm wide and 2.2 μm deep. Deposition condition: $C_2H_5OH[Cu(hfac)_2$:0.146 mol/l] = 4.5 sccm, total flow rate = 90 sccm, 13 Pa, $P_m = 45$ W, $P_{as} = 300$ W, $V_{dc} = -100$ V, and $T_s = 150$ °C.

Resistivity of Cu films

The as-deposited electrical resistivity of 100-nm-thick Cu films was measured by the four-point probe method. The resistivity of Cu films deposited without applying the substrate bias voltage is 1.85 μΩcm, which is close to the Cu bulk resistivity of 1.72 μΩcm. The resistivity of films deposited on the top surface with the bias voltage is ≥4 μΩcm, while that of Cu in trenches has not been evaluated yet. Further reduction of the resistivity is necessary for films deposited by the anisotropic CVD, while the reasons bringing about such relatively high resistivity have not been identified yet.

Identification of ionic species

Identification of ionic species irradiating on the substrate surface is important, since the deposition rate increasing with flux and kinetic energy of ions impinges on it. The mass spectrum of the ionic species was measured with a quadrupole mass spectrometer. Figure 4 shows a typical mass spectrum of Ar + H_2 (11 %) discharge. In spite of low H_2 partial pressure, the signal intensity of H_3^+ ions is the highest and that of ArH^+ is 1/10 of H_3^+, whereas those of H^+, H_2^+, and Ar^+ are below a detection limit of the mass spectrometer. The experimental spectrum is consistent with previous simulation and experiments [19,20], which show H_3^+ and ArH^+ ions are generated by the following fast ion-neutral reactions,

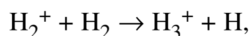

$$H_2^+ + H_2 \rightarrow H_3^+ + H,$$

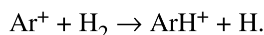

$$Ar^+ + H_2 \rightarrow ArH^+ + H.$$

Thus, H_3^+ is the main ionic species that contributes to the anisotropic deposition. Sputtering by ArH^+ ions probably modifies the deposition profile, since film thickness on the top surface around the entrance of trenches becomes thinner for a lower *R*.

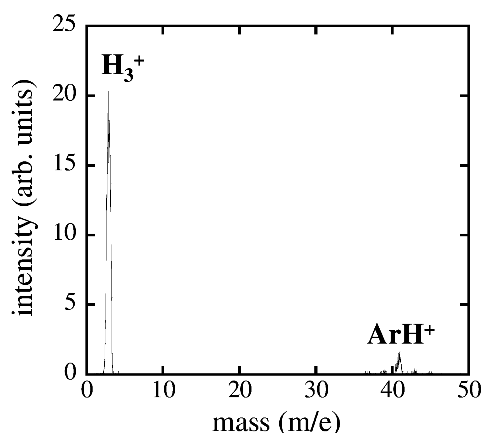

Fig. 4 Typical mass spectrum of Ar + H_2 (11 %) discharge. Experimental conditions: Ar + H_2 (11 %) = 90 sccm, 13 Pa, P_m = 50 W, and P_{as} = 0 W.

Ion density in main discharge

The *R* dependence of ion saturation current was studied using a Langmuir probe in order to obtain information about the ion density in the main discharge. Figure 5 shows the results with the discharge of H atom source (P_{as} on) together with those without the discharge (P_{as} off). The ion saturation current slightly increases with R. Taking into account the fact that H_3^+ ions are predominant, the ion density in the discharge does not significantly change for R = 11–100 %. Furthermore, the current with the discharge of H atom source is nearly the same as that without the discharge, indicating little effects of the discharge of H atom source on the ion density of the main discharge.

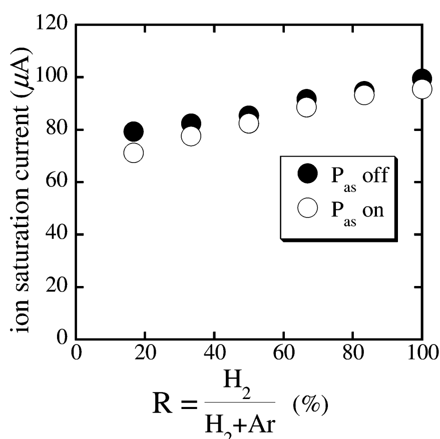

Fig. 5 $R = H_2/(H_2 + Ar)$ ratio dependence of ion saturation current at 12 mm above the center of substrate electrode with discharge of H atom source (P_{as} on) and without it (P_{as} off). Experimental conditions: total flow rate = 90 sccm, 13 Pa, P_m = 45 W, and P_{as} = 300 W.

Emission intensities of H_α and Ar^+ in the main discharge

ArH^+ ions and H atoms play important roles in the Cu anisotropic plasma CVD. ArH^+ ions are expected to sputter Cu deposited on the top surface around the entrance of trenches and, hence, prevent trenches from pinching off their entrance. H atoms are effective in improving qualities of Cu films: (1) removing impurities of C, O, and F in Cu; (2) reducing surface roughness; and (3) increasing size of Cu grains [4–7]. In order to obtain information about these fluxes, emission intensities of H_α 656.28 nm and Ar^+ 514.53 nm in the main discharge, which indicate generation rates of H atoms and Ar^+ ions, respectively, were measured as a function of *R*. Figure 6 shows the results. With increasing *R*, the emission intensity of Ar^+ linearly decreases, whereas that of H_α sharply increases for *R* = 0–33 % and then slightly de-

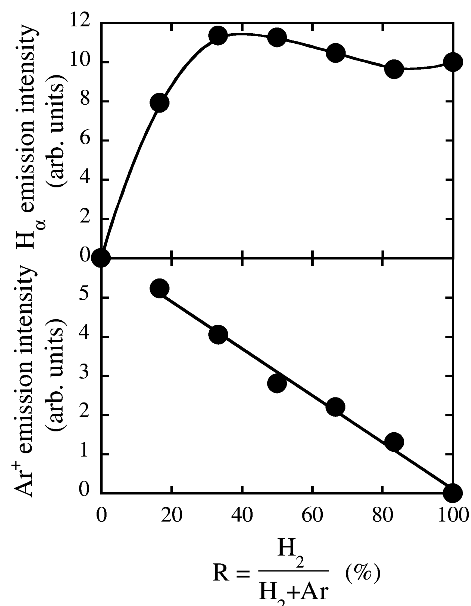

Fig. 6 Dependence of H_α and Ar^+ 514.53 nm intensities on ratio $R = H_2/(H_2 + Ar)$. Experimental condition: total flow rate = 90 sccm, 24 Pa, P_m = 45 W, and P_{as} = 300 W.

creases for R = 33–100 %. The generation rate of Ar^+ ions is closely related with that of ArH^+, since ArH^+ is generated by the fast reaction between Ar^+ and H_2. Therefore, the sputtering due to ArH^+ is expected to be enhanced by reducing R, while a high H flux is obtained for R = 33–100 %.

A tentative model for anisotropic deposition

Here, we focus our attention on anisotropic deposition, since we have already discussed the mechanism bringing about subconformal and conformal depositions [7]. We consider the mechanism for anisotropic deposition dividing into two parts of nucleation of Cu and subsequent film growth.

Nucleation of Cu is initiated by adsorption and subsequent chemisorption of Cu-containing radicals [dominantly Cu(hfac)], followed by impurity reduction due to reactions of H atoms. *Sputtering due to* H_3^+ *and* ArH^+ *tends to suppress the nucleation, because it enhances desorption of adsorbed species.* Since the sputtering rate is the maximum at an incident angle of 20° [2,3] and the flux density of ions irradiating the top surface is higher than that doing the bottom, the nucleation on the bottom takes place faster than that on the top surface. However, the sputtering is difficult to suppress the nucleation on the sidewall, because its rate becomes small for an incident angle above 60° [2,3] and the flux density of ions on the sidewall is also small. We need further study to identify the mechanism to explain the suppression of nucleation on the sidewall.

Once nucleation of Cu takes place, Cu is hard to be etched [21], especially for a low T_s of 130–150 °C employed in our experiments. As already shown, the deposition rate significantly increases with increasing the flux and kinetic energy of ions after the nucleation. In other words, *the ion irradiation enhances Cu deposition once nucleation takes place.* In this phase, the deposition rate is expressed as

(deposition rate) = (deposition rate due to ion-enhanced CVD)
+ (deposition rate due to CVD)
– (sputtering rate).

Our tentative model indicates that control of nucleation of Cu is important to realize the anisotropic deposition. However, an additional mechanism is necessary for explaining the suppression of nucleation on the sidewall. Experiments to reveal such mechanism are underway.

CONCLUSIONS

By using HAPCVD, we have demonstrated not only conformal and subconformal deposition profiles in trenches, but also an anisotropic one. The key to control of the deposition profile is ion irradiation. With increasing the flux and energy of ions, the profile changes from conformal to subconformal and then to an anisotropic one. H_3^+ ions play a major role to the anisotropic CVD, while ArH^+ ions also contribute to modifying the deposition profile. We are now carrying out further experiments for studying the anisotropic deposition more in details.

ACKNOWLEDGMENTS

This research was supported partly by a Grant-in-Aid for Scientific Research (B) from the Japan Society for the Promotion of Science. We are indebted to Prof. S. Samukawa, Tohoku University and Dr. G. Chung, Tokyo Electron Ltd., for supplying Si substrates with trenches. We would like to acknowledge the assistance of Messrs. H. Matsuzaki and T. Kinoshita who contributed greatly to the preparation of the experimental set-up.

REFERENCES

1. G. Timp. *Nanotechnology*, p. 1, Springer Verlag, New York (1998).
2. C. F. Abrams and D. B. Graves. *IEEE Trans. Plasma Sci.* **27**, 1426 (1999).
3. D. Zhang, P. J. Stout, P. L. G. Ventzek. *J. Vac. Sci. Technol.* **A21**, 265 (2003).
4. H. J. Jin, M. Shiratani, Y. Nakatake, T. Fukuzawa, T. Kinoshita, Y. Watanabe, M. Toyofuku. *Jpn. J. Appl. Phys.* **38**, 4492 (1999).
5. H. J. Jin, M. Shiratani, T. Kawasaki, T. Fukuzawa, T. Kinoshita, Y. Watanabe, H. Kawasaki, M. Toyofuku. *J. Vac. Sci. Technol.* **A17**, 726 (1999).
6. H. J. Jin, M. Shiratani, Y. Nakatake, K. Koga, T. Fukuzawa, T. Kinoshita, Y. Watanabe. *Res. Rep. Inf. Sci. Electron. Eng. Kyushu Univ.* **5**, 57–61 (2000).
7. M. Shiratani, H. J. Jin, K. Takenaka, K. Koga, T. Kinoshita, Y. Watanabe. *Sci. Technol. Adv. Mater.* **2**, 505 (2001).
8. K. Takenaka, H. J. Jin, K. Koga, M. Onishi, M. Shiratani, Y. Watanabe. *Proc. of Int. Symp. on Dry Process*, pp. 169–174, Institute of Electrical Engineering of Japan, Tokyo (2002).
9. K. Takenaka, M. Onishi, T. Kinoshita, K. Koga, M. Shiratani, Y. Watanabe, T. Shingen. *Proc. of Int. Workshop on Informations & Electrical Engineering*, p. 227, Suwon, Korea (2002).
10. S. Kim, D. J. Choi, K. R. Yoon, K. H. Kim, S. K. Koh. *Thin Solid Films* **311**, 218 (1997).
11. Y. S. Kim, D. Jung, D. J. Kim, S. K Min. *Jpn. J. Appl. Phys.* **37**, L991 (1998).
12. N. I. Cho and Y. Sul. *Mater. Sci. Eng.* **B72**, 184 (2000).
13. K. Weiss, S. Riedel, S. E. Schulz, M. Helneder, H. Wendt, T. Gessner. *Microelectron. Eng.* **50**, 433 (2000).
14. J. A. T. Norman. *J. Phys. IV* **11**, Pr3-497 (2001).
15. Y. K. Chae and H. Komiyama. *J. Appl. Phys.* **90**, 3610 (2001).
16. S. K. Kwak, K. S. Chung, I. Park, H. Lim. *Curr. Appl. Phys.* **2**, 205 (2002).
17. C. L. Lin, P. S. Chen, M. C. Chen. *J. Vac. Sci. Technol.* **B20**, 1111 (2002).
18. K. Takenaka, M. Shiratani, M. Onishi, M. Takeshita, T. Kinoshita, K. Koga, Y. Watanabe. *Mater. Sci. Semiconduct. Process.* **5**, 301 (2003).
19. Y. Watanabe, M. Shiratani, S. Ogi, N. Kunihiro, I. Ogawa. *Jpn. J. Appl. Phys.* **27**, 1469 (1988).
20. A. Bogaerts and R. Gijbels. *Phys. Rev. E* **65**, 054602 (2002).
21. B. J. Howard and Ch. Steinbrüchel. *Appl. Phys. Lett.* **59**, 914 (1991).